Bull. Mater. Sci., Vol. 36, No. 6, November 2013, pp. 1005–1011. © Indian Academy of Sciences.

# Influence of conductive electroactive polymer polyaniline on electrochemical performance of $LiMn_{1\cdot95}Al_{0\cdot05}O_4$ cathode for lithium ion batteries

**CHANG-LING FAN***, **HARI OM**[†], **KE-HE ZHANG and SHAO-CHANG HAN**
College of Materials Science and Engineering, Hunan University, Changsha 410082, P. R. China
[†]Department of Materials Science and Engineering, Indian Institute of Technology, Kanpur 208 016, India

MS received 14 April 2012; revised 2 August 2012

**Abstract.** **Conductive electroactive polymer polyaniline is utilized to substitute conductive additive acetylene black in the $LiMn_{1\cdot95}Al_{0\cdot05}O_4$ cathode for lithium ion batteries. Results show that $LiMn_{1\cdot95}Al_{0\cdot05}O_4$ possesses stable structure and good performance. Percolation theory is used to optimize the content of conductive additive in cathode. It shows that the conductivity of cathode reaches its maximum value when the content of conductive additives is 15 wt%. This is in agreement with the results of charge and discharge experiments. The application of polyaniline can evidently enhance the electrochemical performance of cathode. The discharge capacity of cathode using 15 wt% polyaniline is 95·9 mAh $g^{-1}$ at the current density of 170 mA $g^{-1}$. The charge transfer resistance under different depths of discharge of cathode is much lower compared with the use of acetylene black. It can be concluded that the application of polyaniline in cathode can greatly improve the electrochemical performances of $LiMn_{1\cdot95}Al_{0\cdot05}O_4$ cathode.**

**Keywords.** **Lithium ion batteries; polyaniline; $LiMn_{1\cdot95}Al_{0\cdot05}O_4$; percolation theory; electrochemical performances.**

## 1. Introduction

Spinel $LiMn_2O_4$ possesses several advantages such as abundant raw materials, low price, small toxicity, high potential platform and environmental friendly. Therefore, it is one of the most potential candidate cathodes to replace $LiCoO_2$ in lithium ion batteries. However, its utilization has been hindered by the Jahn–Teller effect, dissolution of Mn and decomposition of electrolyte. Cations such as $Al^{3+}$ (Kakuda *et al* 2007; Xiao *et al* 2008), $Co^{2+}$ (Sakunthala *et al* 2010), $Ni^{2+}$ (Li *et al* 2009), $Cr^{3+}$ (Thirunakaran *et al* 2005), $La^{3+}$ (Arumugam *et al* 2008), $Zn^{2+}$ and $Ce^{4+}$ (Arumugam and Kalaignan 2010) have been used to stabilize the spinel structure, suppress the Jahn–Teller effect and improve its cycle performances.

$LiMn_2O_4$ is a semiconductor and its conductivity is as low as $5{\cdot}69 \times 10^{-5}$ S $cm^{-1}$ (Fan *et al* 2011). The coating of conductive materials on its surfaces such as gold (Tu *et al* 2006), silver (Son *et al* 2004; Zhou *et al* 2008), aluminum (Li and Xu 2007) and carbon (Yue *et al* 2009), has been utilized to enhance its electrochemical performances. However, these inert substances do not possess capacity.

Owing to the fact that they are easy to synthesize and have high conductivity and good environmental stability, conductive electroactive polymers, polypyrrole and polyaniline (PAn), receive a lot of attention. Several reports have referred to their applications in $LiMn_2O_4$ cathode. *In situ* (Kuwabata *et al* 1999; Pasquier *et al* 1999) and *ex situ* (Kim *et al* 2001) chemical polymerization has been utilized to fabricate the cathode of $LiMn_2O_4$ and polypyrrole to enhance the electrochemical performances. PAn has also been used to modify $LiMn_2O_4$ and improve its performances by *in situ* electrochemical (Li *et al* 2004) and *ex situ* chemical polymerization method (Fonseca and Neves 2004). However, strong acidity and oxidant of the polymerization system will destroy the surface crystallite structure of $LiMn_2O_4$ and deteriorate its performance. To the best of our knowledge, the relationships between the content of conductive PAn and electrochemical performances of $LiMn_2O_4$ cathode are a few.

In this paper, $Al^{3+}$-doped $LiMn_2O_4$ was prepared by solid state reaction method. PAn synthesized with high conductivity of 15·29 S $cm^{-1}$ was utilized to replace acetylene black (AB), which is commonly used as conductive additive in $LiMn_2O_4$ cathode. Percolation theory was applied to discuss the relationships between conductivity of $LiMn_2O_4$ cathode and content of conductive additives, PAn and AB. The electrochemical performances of $LiMn_2O_4$ cathode were systematically investigated when 15 wt% PAn was used to replace AB.

## 2. Experimental

### 2.1 *Preparation of samples*

$LiMn_{1\cdot95}Al_{0\cdot05}O_4$ was synthesized by liquid phase mixing and solid-state reaction. Lithium carbonate, manganese

*Author for correspondence (clfanhd@yahoo.com.cn)

dioxide and aluminum nitrate nanohydrate were homogeneously blended at the atomic ratio of 1:1·95:0·05 (Li:Mn:Al). The mixture was preheated at 650 °C for 5 h and further calcinated at 750 °C for 12 h in air. Conductive electroactive polymer, PAn, was synthesized by a chemical oxidative method as described elsewhere (Fan *et al* 2011). It was prepared in the media of hydrochloric acid and ammonium persulfate was used as oxidant.

### 2.2 *Sample characterization*

X-ray diffraction (XRD) was performed on D-MAX2500VB diffractometer (Rigaku Co., Japan). The morphology was investigated by JSM-6700F scanning electron microscopy (SEM, Japan Electronic Co., Japan). Particle sizes were determined with a JL-1177 laser granularity tester (Jingxin Co., China) by using ionized water as solvent. Fourier transform infrared spectroscopy (FTIR) was determined with a Nicolet 6700 (Thermo Fisher Scientific Co., USA). The electronic conductivity of powder and film samples was determined at a pressure of 4·90 MPa with two-electrode method. It was conducted by connecting a GM-II resistivity tester (Coal Chemistry Institute, China) and a 34401A type 6 1/2 Digit multimeter (Agilent Co., USA).

### 2.3 *Preparation of cathode films and cell*

Cathode films with a thickness of 0·1 mm were prepared by mixing $LiMn_{1\cdot95}Al_{0\cdot05}O_4$ with PAn and AB and binder polytetrafluoroethylene (PTFE). The mass content of PTFE was kept at 5 wt%. The films were dried in a vacuum oven at 70 °C for 24 h. Three electrode cells were utilized to determine the electrochemical performances. The lithium foils were used as counter and reference electrodes. A microporous polymer separator, Celgard 2400, was utilized (Celgard Co., USA). The electrolyte used was 1 mol $L^{-1}$ $LiPF_6$ having a mixture of ethylene carbonate, dimethylene carbonate and ethyl methyl carbonate (1:1:1, v:v:v) (Tinci Co., China). Cells were assembled in a glove box filled with ultra purity argon gas.

### 2.4 *Characterization of electrochemical performances*

The charge and discharge performances were examined by a BT2000 battery testing system (Arbin Co., USA) at various current densities in the range of 3·300–4·300 V (vs $Li^+$/Li). Electrochemical impedance spectra and cyclic voltammetry were performed by using a CHI 660c electrochemical workstation (Chenhua Co., China). The amplitude of potential was 5 mV and frequency was from 100 kHz to 0·01 Hz. The potential scan rate of cyclic voltammetry was 0·1 mV $s^{-1}$.

## 3. Results and discussion

### 3.1 *Structure and performance of $LiMn_{1\cdot95}Al_{0\cdot05}O_4$*

XRD patterns of $LiMn_{1\cdot95}Al_{0\cdot05}O_4$ and standard $LiMn_2O_4$ are presented in figure 1. The main peaks are labelled with

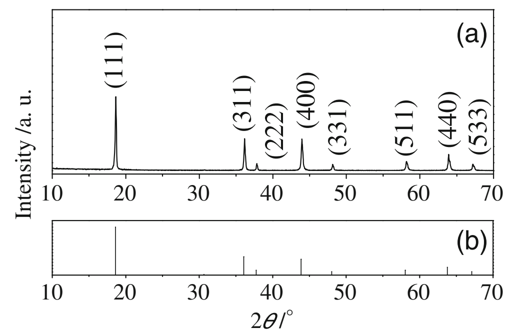


**Figure 1.** XRD pattern of $LiMn_{1\cdot95}Al_{0\cdot05}O_4$ (**a**) and standard $LiMn_2O_4$ (**b**).

*hkl* indices. As can be seen from the figure 1, it is in consistence with the standard spectrum (35-0782). All peaks belong to spinel phase and there is not any impurity. It indicates that $LiMn_{1\cdot95}Al_{0\cdot05}O_4$ possesses typical spinel structure. The intensity ratio of (311) to (400) is 1·04. It indicates that $LiMn_{1\cdot95}Al_{0\cdot05}O_4$ will possess good electrochemical performances according to literature (Lee *et al* 2001).

The lattice parameter of $LiMn_{1\cdot95}Al_{0\cdot05}O_4$ (0·8229 nm) is very close to that of the standard spinel, $LiMn_2O_4$ (0·8247 nm) (He *et al* 2007). Therefore, its crystallite volume (0·5572 $nm^3$) is smaller than that of the standard spinel (0·5609 $nm^3$). This is because the radius of $Al^{3+}$ (0·053 nm) is much smaller than that of $Mn^{3+}$ (0·066 nm) and $Mn^{4+}$ (0·060 nm). The bond energy of the Al–O (512 kJ $mol^{-1}$) is greater than that of Mn–O (402 kJ $mol^{-1}$). Therefore, the crystallite unit shrinks and the stability of spinel structure increases.

Two potential plateaus exist in the discharge curve of $LiMn_{1\cdot95}Al_{0\cdot05}O_4$. This means that lithium ions will intercalate at two kinds of positions (He *et al* 2007). It is the typical feature of spinel $LiMn_2O_4$. Its discharge capacity is 104·2 mAh $g^{-1}$, which is near to its common capacity of 110 mAh $g^{-1}$.

### 3.2 *Structure and performance of PAn*

The electronic conductivity of AB, which is commonly utilized as conductive additive, is as low as 7·77 S $cm^{-1}$. The conductive additive with high conductivity should be selected to enhance the electrochemical performances of $LiMn_{1\cdot95}Al_{0\cdot05}O_4$. Conductive electroactive polymer PAn is synthesized with optimal conditions of chemical oxidative method. The FTIR spectrum of PAn is illustrated in figure 2.

The peaks at 1573 and 1493 $cm^{-1}$ belong to quinoid and benzenoid ring-stretching deformations, respectively. The absorption bands at 1373 and 1301 $cm^{-1}$ are assigned to *p*-electron delocalization in PAn induced by protonation. The characteristic peak of protonated PAn is at 1240 $cm^{-1}$ and can be looked as a C–$N^{+\bullet}$ stretching vibration in the polaron structure. The 1134 $cm^{-1}$ peak corresponds to a vibration of –$NH^{\bullet+}$ structure. The out-of-plane deformations of C–H on rings are located at 800 $cm^{-1}$. Therefore, PAn prepared possesses typical features of conductive emeraldine salts. The conductivity of PAn prepared under optimal conditions is 15·29 S $cm^{-1}$. Its $d_{50}$ value of granularity distribution is 0·353 $\mu$m, which is very near to the 0·448 $\mu$m of AB. Therefore, PAn possesses similar granularities and can be utilized as conductive additive.

Galvanostatic charge and discharge curves and cyclic voltammograms of PAn in the 1st cycle and 20th cycle are given in figure 3. From the figure, we find that there is no evidently potential platform in the charge and discharge process. The cyclic voltammograms also show that there is no oxidation and reduction peak. These are very similar to the phenomenon of super capacitor. The discharge capacity of PAn is 45·6 mAh $g^{-1}$ in the first cycle. The capacity declines very slowly in 20 cycles according to cyclic voltammograms.

The charge and discharge process can be explained by the formula:

$$[\mathrm{PAn}^0] - e + \mathrm{PF}_6^- \xleftrightarrow{\text{charge/discharge}} [\mathrm{PAn}^+]\mathrm{PF}_6^-. \quad (1)$$

During the charge process, PAn loses its electrons and $PAn^+$ cations are formed. Then, $PF_6^-$ anions from electrolyte will combine with PAn chains at its cations vacant to neutralize the molecule chains. In the discharge process, when $PAn^+$ receives electrons to form PAn, the combined anions $PF_6^-$ will leave and go back to electrolyte to hold electric neutrality. Therefore, PAn can be used as cathode active material. The charge carriers are $PF_6^-$ anions but not $Li^+$ cations.

The conductivity of PAn prepared is 15·29 S $cm^{-1}$. Its value will change with the increase (or decrease) of the potential of PAn cathode. In the charge process, PAn loses its electrons and $PAn^+$ is formed. $PF_6^-$ anions from electrolyte will combine with $PAn^+$ chain gradually at its cations vacant. This process is the so-called 'doping of PAn with $PF_6^-$'. It is well known that the doping of conductive polymer PAn with electron donors (anions) is the introduction of electrons into the conduction band. The increasing of electrons content in conduction band will cause the rise of its conductivity. It shows that the conductivity of PAn will increase gradually in the charge process. In the discharge process, $PF_6^-$ anions combined with PAn will leave and the electrons in the conduction band decrease at the same time. Therefore, its conductivity drops step by step and reaches its original value at the end of discharge process. It can be concluded that the conductivity of PAn will be larger than the value of 15·29 S $cm^{-1}$ in the charge and discharge operations.

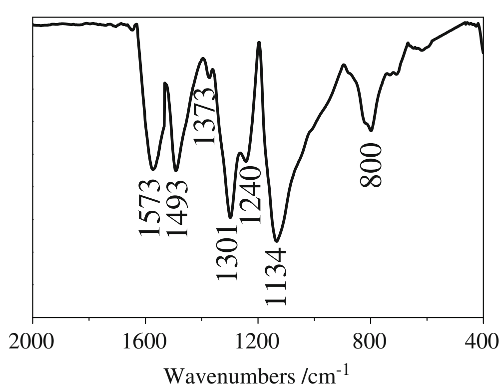


**Figure 2.** FTIR spectrum of PAn.

### 3.3 *Percolation theory analysis*

The conductivity of $LiMn_2O_4$ is as low as $5{\cdot}69 \times 10^{-5}$ S $cm^{-1}$. Conductive additives must be added to enhance its electrochemical performances. The commonly used conductive additive AB possesses a low conductivity of 7·77 S $cm^{-1}$. In this paper, the prepared conductive polymer PAn, whose conductivity (15·29 S $cm^{-1}$) is much larger than that of AB, is applied to substituted AB to improve the conductivity of cathode film and the electrochemical performances of cathode $LiMn_{1{\cdot}95}Al_{0{\cdot}05}O_4$. Furthermore, the discharge capacity of PAn can also contribute to the improvement of electrochemical performance of cathode.

The minimum required content of conductive additive in cathode polymer should be obtained to minimize the content of inert materials and improve the specific capacity of cathode. The conductivities of $LiMn_{1{\cdot}95}Al_{0{\cdot}05}O_4$ cathode with different volume percentages of conductive additives, PAn and AB, are illustrated in figure 4. The mass content of PTFE in cathode is kept at 5 wt%. The conductivities of $LiMn_{1{\cdot}95}Al_{0{\cdot}05}O_4$ cathode with various mass contents of PAn

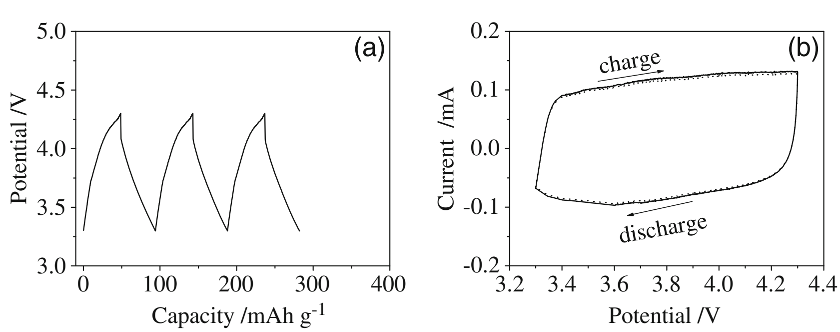


**Figure 3.** Galvanostatic charge and discharge curves (**a**) and cyclic voltammograms (**b**) of PAn in 1st cycle (solid line) and 20th cycle (dotted line).

and AB (5, 10, 15 and 20 wt%) are also presented. The conductivity of cathode increases only a little when the volume percentage of PAn and AB increases from 0 to 2·50%. When the volume percentage reaches 5·00%, the conductivity of $LiMn_{1\cdot 95}Al_{0\cdot 05}O_4$ film begins to increase obviously. This content is the so-called 'percolation threshold'. The conductivity of $LiMn_{1\cdot 95}Al_{0\cdot 05}O_4$ cathode will not increase evidently with the increase of the content of conductive additive when the mass content of PAn and AB reaches 15 wt%. Under this condition, the amounts of conductive additive particle in cathode are enough to form a workable conductive network. It can be concluded that the transformations of conductivity of cathode conform to the percolation theory. The conductivity of $LiMn_{1\cdot 95}Al_{0\cdot 05}O_4$ cathode with 15 wt% PAn is as high as $8\cdot 19 \times 10^{-1}$ S $cm^{-1}$. Note that the conductivity of $LiMn_{1\cdot 95}Al_{0\cdot 05}O_4$ cathode containing PAn is much bigger than that of cathode utilizing AB.

The scaling law (2) is often employed to analyse the percolation behaviour of conductive polymer composite (Martin *et al* 2004):

$$\sigma \propto (P - P_c)\exp(t)\,, \tag{2}$$

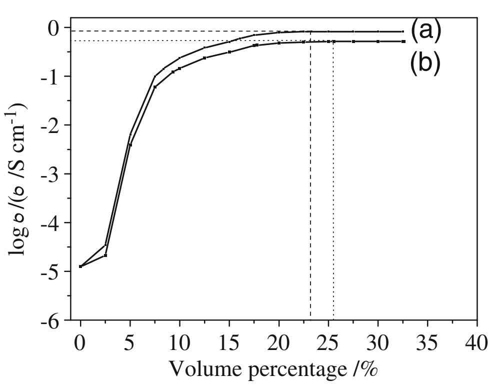


**Figure 4.** Dependence of conductivities of $LiMn_{1\cdot 95}Al_{0\cdot 05}O_4$ cathode composite on volume percentage of PAn (**a**) and AB (**b**).

where $\sigma$ in the equation represents conductivity of $LiMn_{1\cdot 95}Al_{0\cdot 05}O_4$ cathode, $P_c$ and $P$ are the critical and actual content of conductive additive. $t$ is the conductivity exponent and its value generally reflects the dimensionality of the filler network in conductive composite. Its typical value is between 1·6 and 2·0 for three dimensions composite. The results in figure 4 is to be fitted according to the variation of log $\sigma(\sigma/\mathrm{S\ cm^{-1}})$ with $\log(P-P_c)((P-P_c)/\%)$. After calculation, we obtained the exponent $t$ of $LiMn_{1\cdot 95}Al_{0\cdot 05}O_4$ cathode which were 1·10 and 1·03 when PAn and AB were used. It should be noted that the $LiMn_{1\cdot 95}Al_{0\cdot 05}O_4$ cathode discussed here is quite different from conductive polymer composite in literature. The content of polymer in the latter is 80–90 wt%. However, the content of polymer PTFE in cathode is only 5 wt%. Hence, it is reasonable that the difference exists between the $t$ value obtained here and the typical value in literature.

### 3.4 *Rate performance*

Figures 5 and 6 present the discharge capacities and curves of $LiMn_{1\cdot 95}Al_{0\cdot 05}O_4$ cathode with various contents of PAn and AB at different current densities. From the figures, we find that the rate performance of $LiMn_{1\cdot 95}Al_{0\cdot 05}O_4$ cathode increases with increase in the mass content of conductive additive. When the content of PAn and AB reaches 15 wt%, the rate performance of $LiMn_{1\cdot 95}Al_{0\cdot 05}O_4$ cathode reaches stable state. It does not increase evidently when the content increases to 20 wt%. This is in accordance with the conductivity analysis. The discharge capacities of $LiMn_{1\cdot 95}Al_{0\cdot 05}O_4$ cathode using 15 wt% AB are also given in the figures for comparison.

When 15 wt% AB is utilized, the discharge capacity of $LiMn_{1\cdot 95}Al_{0\cdot 05}O_4$ cathode decreases obviously and its potential profile drops very quickly with the increase of current density. The discharge capacity is only 66·3 mAh $g^{-1}$ when current density reaches 170 mA $g^{-1}$.

However, rate performance of $LiMn_{1\cdot 95}Al_{0\cdot 05}O_4$ cathode is greatly improved when 15 wt% PAn is used. The

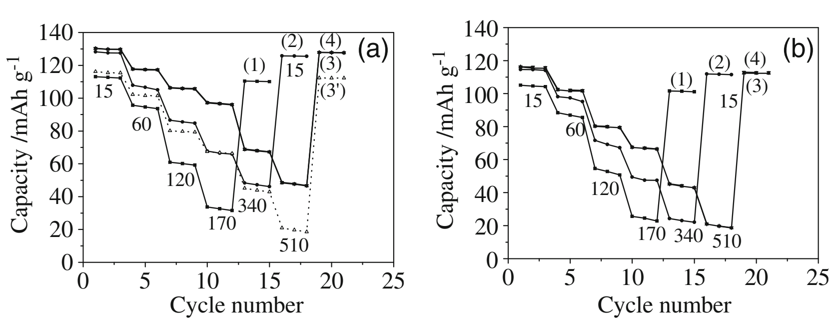


**Figure 5.** Discharge capacities of $LiMn_{1\cdot 95}Al_{0\cdot 05}O_4$ cathode composite under different current densities using various mass content of PAn (**a**) and AB (**b**) as conductive additive. Dotted line (3′) in (**a**) is that of $LiMn_{1\cdot 95}Al_{0\cdot 05}O_4$ cathode composite containing 15 wt% AB. (1) 5 wt%; (1) 10 wt%; (3) 15 wt% and (4) 20 wt%. Numbers in figures are their corresponding current density with unit of mA $g^{-1}$.

discharge capacity of $LiMn_{1.95}Al_{0.05}O_4$ cathode decreases very slowly with a increase of current density. The discharge capacity is as high as 95·9 mAh $g^{-1}$ at a current density of 170 mA $g^{-1}$. When the current density reaches 510 mA $g^{-1}$, the discharge capacity of $LiMn_{1.95}Al_{0.05}O_4$ cathode containing PAn is 46·5 mAh $g^{-1}$. This is 27·9 mAh $g^{-1}$ higher than that of cathode using AB. Therefore, the rate performance of $LiMn_{1.95}Al_{0.05}O_4$ cathode improves when PAn is used.

We know that the conductivity of $LiMn_{1.95}Al_{0.05}O_4$ cathode film containing 15 wt% PAn ($8{\cdot}19 \times 10^{-1}$ S $cm^{-1}$) is 58% larger than that of cathode containing 15 wt% AB ($5{\cdot}16 \times 10^{-1}$ S $cm^{-1}$). Therefore, the polarization degree of cathode in charge and discharge processes decreases when AB is replaced with the same content of PAn. Hence, the utilization ratio of active material $LiMn_{1.95}Al_{0.05}O_4$ in cathode is improved. It is understandable that the electrochemical performances of cathode are enhanced when PAn is used. Furthermore, compared with the inert conductive additive AB in the potential range of cathode, the discharge capacity of PAn can also help to increase the discharge capacity of cathode under different current densities.

### 3.5 *Electrochemical impedance spectra*

Electrochemical impedance spectra of $LiMn_{1.95}Al_{0.05}O_4$ cathode at different depths of discharge in the third cycle using 15 wt% PAn and AB are shown in figure 7. Two semicircles and a straight line exist and this is in agreement with literature (Park *et al* 2001; Zhou *et al* 2006). The equivalent circuit used to fit the spectra is also given in the figure. $R_s$ represents the electrolyte resistance. $R_f$ and $R_{ct}$ are assigned to the resistance of Li migration through surface passive film and the charge transfer resistance, respectively. $CPE_1$ and $CPE_2$ (constant phase elements) are used to describe the non-ideal behaviours of the surface film and the interface of film solution. $Z_w$ is associated with the diffusion process of Li ions in the solid phase of $LiMn_{1.95}Al_{0.05}O_4$.

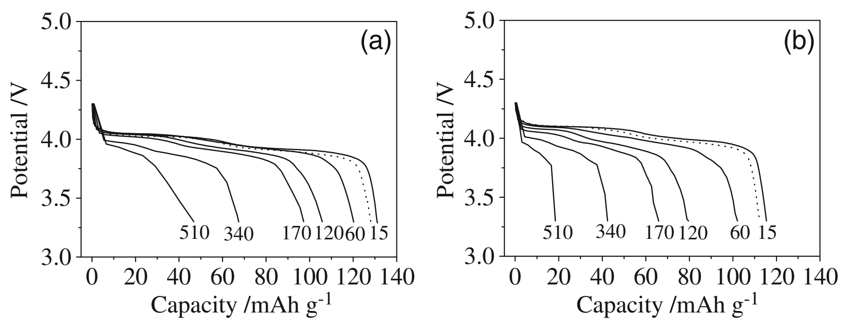


**Figure 6.** Discharge curves of $LiMn_{1.95}Al_{0.05}O_4$ cathode composite in third cycle under different current densities containing 15 wt% PAn (**a**) and AB (**b**). Numbers in figures are their corresponding current density with unit of mA $g^{-1}$.

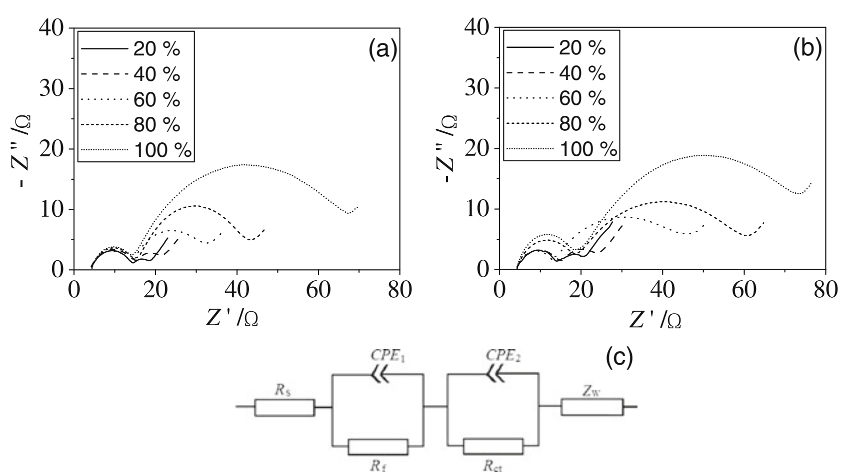


**Figure 7.** Electrochemical impedance spectra of $LiMn_{1.95}Al_{0.05}O_4$ cathode at different depths of discharge containing 15 wt% PAn (**a**) and AB (**b**) and equivalent circuit (**c**).

**Table 1.** Equivalent circuit elements of cathode containing 15 wt% PAn and AB.

| Cathode containing | DOD (%) | $R_s$ (Ω) | $R_f$ (Ω) | $R_{ct}$ (Ω) | $Z_w$ (Ω) |
|---|---|---|---|---|---|
| PAn | 20 | 4·19 | 10·41 | 3·91 | 0·0518 |
| | 40 | 4·21 | 10·56 | 6·62 | 0·0530 |
| | 60 | 4·22 | 10·65 | 16·89 | 0·0572 |
| | 80 | 4·24 | 10·76 | 25·44 | 0·0611 |
| | 100 | 4·26 | 10·82 | 54·90 | 0·0752 |
| AB | 20 | 4·41 | 10·61 | 5·68 | 0·0522 |
| | 40 | 4·45 | 10·76 | 8·32 | 0·0534 |
| | 60 | 4·47 | 10·83 | 29·67 | 0·0631 |
| | 80 | 4·48 | 14·56 | 38·25 | 0·0669 |
| | 100 | 4·51 | 14·62 | 58·19 | 0·0760 |

All the fitting results of cathode under different depths of discharge are given in table 1. It is found that the charge transfer resistance of cathode increases gradually with the increase of depth of discharge. The changes of $Z_w$ also have similar tendency. This is because the concentration of lithium ions in crystallite and repulsive forces between lithium ions will increase with the increase of depth of discharge. Therefore, resistance increases when more lithium ions enter into it.

As can be seen from table 1, the charge transfer resistance of cathode is much lower when PAn is used to replace AB. We know that the charge and discharge processes in cathode are conducted through the intercalation and de-intercalation of lithium ions in cathode active materials which are surrounded by conductive network. At the same time, electrons are transferred between the current collectors and conductive network. In this paper, the conductivity of cathode film containing PAn is much higher than that of using AB. Hence, speed of intercalation (de-intercalation) of lithium ions and transfer of electrons in cathode increase when PAn is used as conductive additive. Therefore, the charge and discharge, i.e. the charge transfer process will be faster. Hence, the exchange current density will be larger. Then, the charge transfer resistance of cathode containing PAn will be much lower than that of AB under different depths of discharge.

It can also be found that the electrolyte resistance of $LiMn_{1·95}Al_{0·05}O_4$ cathode remains nearly unchanged under different depths of discharge. The gaps between different cathodes are also very small. When PAn is used as conductive film, the resistance change of surface passive film of cathode is very small with the rise of depth of discharge. However, the surface film resistance increases obviously from 10·61 to 14·62 Ω when AB is utilized. It indicates that the surface passive film of cathode containing PAn is steadier than that of cathode using AB.

### 3.6 *Cycle performance*

The discharge capacities of $LiMn_{1·95}Al_{0·05}O_4$ cathode containing 15 wt% PAn and AB as a function of cycle number are shown in figure 8. It can be seen that when 15 wt% PAn is used, the discharge capacity of cathode decreases slowly from 130·3 to 127·8 mAh $g^{-1}$. The retention ratio of capacity is as high as 98·08% in 50 cycles. However, discharge capacity of cathode declines gradually from 116·2 to 111·3 mAh $g^{-1}$ when AB is added as conductive additive. Its retention percentage is only 95·78% which is lower than 98·08%. It can be concluded that $LiMn_{1·95}Al_{0·05}O_4$ cathode possesses superior cycle performance when PAn is used as a conductive additive compared to AB.

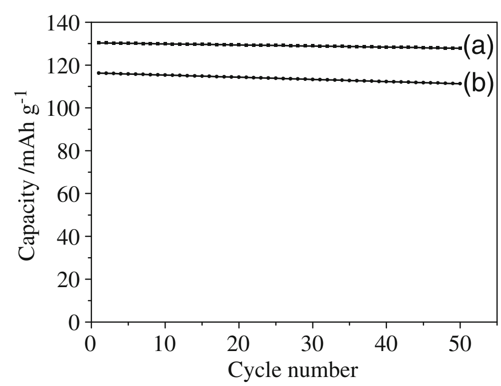


**Figure 8.** Discharge capacity of $LiMn_{1·95}Al_{0·05}O_4$ cathode using 15 wt% PAn (**a**) and AB (**b**) as a function of cycle number.

Figure 9 shows electrochemical impedance spectra of $LiMn_{1·95}Al_{0·05}O_4$ cathode using 15 wt% PAn and AB in the full charge state in the 2nd cycle and the 50th cycle. There is only a little change in the middle frequency semicircle for cathode after 50 cycles when PAn is utilized. On the other hand, the cathode using AB as a conductive additive exhibits a drastic increase of charge transfer resistance from 58·19 to 66·81 Ω in 50th cycle. Therefore, compared with AB, $LiMn_{1·95}Al_{0·05}O_4$ cathode utilizing PAn as a conductive additive shows less impedance growth and could sustain its excellent cycle stability. The conductivity of cathode film containing PAn is $8·19 \times 10^{-1}$ S $cm^{-1}$. This is 58% larger than that of cathode containing AB. This lowers the polarization degree of cathode. PAn belongs to one kind of conductive

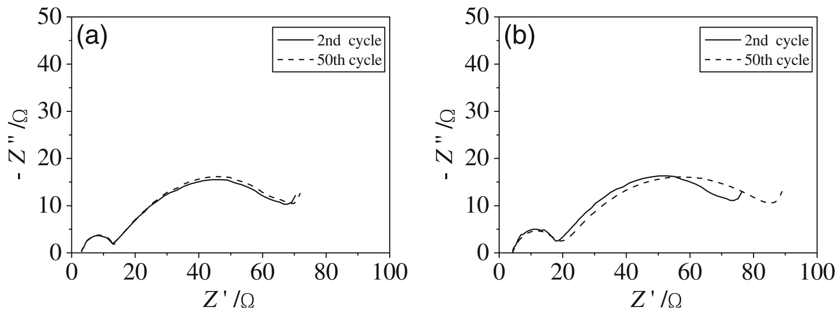


**Figure 9.** Electrochemical impedance spectra of $LiMn_{1·95}Al_{0·05}O_4$ cathode in full charge state using 15 wt% PAn (**a**) and AB (**b**) as conductive additives.

polymers and possesses excellent resiliency. The discharge of the conductive network of cathode is depressed. Therefore, the cathode film can maintain its integrity with the increase of cycle number.

## 4. Conclusions

$LiMn_{1·95}Al_{0·05}O_4$ possesses well developed crystallite structure. The high conductivity of PAn (15·29 S $cm^{-1}$) and its granularity similar to that of AB make it a conductive additive capable of replacing AB. The relationships between conductivities of $LiMn_{1·95}Al_{0·05}O_4$ cathode and volume percentages of conductive additive conform to the percolation theory. The conductivity and discharge capacity of $LiMn_{1·95}Al_{0·05}O_4$ cathode reach their maximum values when the mass content of PAn and AB reaches 15 wt%. The discharge capacity of $LiMn_{1·95}Al_{0·05}O_4$ cathode is enhanced when PAn is used to replace AB, which is as high as 95·9 mAh $g^{-1}$ under 170 mA $g^{-1}$. The cycle performance of cathode is also enhanced. The charge transfer resistance of cathode at different depths of discharge decreases compared to that of using AB. The improvements of the electrochemical performance of cathode using conductive polymer PAn as conductive additive come from high conductivity of 15·29 S $cm^{-1}$ and its excellent resiliency.

## Acknowledgements

The authors would like to thank the National Natural Science Foundation of China (50972044, 51172068) for its financial support. This paper is also supported under the Young Teachers' Growth Plan of Hunan University.

## References

Arumugam D and Kalaignan G P 2010 *J. Electroanal. Chem.* **648** 54

Arumugam D, Kalaignan G P and Manisankar P 2008 *Solid State Ionics* **179** 580

Arumugam D, Vediappan K and Lee C W 2010 *Electrochim. Acta* **55** 8439

Fan C L, Xu Z Y and Su Y C 2011 *Chin. J. Nonferr. Met.* **21** 796

Fonseca C P and Neves S 2004 *J. Power Sources* **135** 249

He B L, Zhou W J, Bao S J, Liang Y Y and Li H L 2007 *Electrochim. Acta* **52** 3286

Kakuda T, Uematsu K, Toda K and Sato M 2007 *J. Power Sources* **167** 499

Kim J U, Jeong I S, Moon S I and Gu H B 2001 *J. Power Sources* **97–98** 450

Kuwabata S, Masui S and Yoneyama H 1999 *Electrochim. Acta* **44** 4593

Lee Y S, Kumada N and Yoshi M 2001 *J. Power Sources* **96** 376

Li X F and Xu Y L 2007 *Electrochem. Commun.* **9** 2023

Li R G, Wang L, Chen M Z and Deng Z H 2004 *Chin. J. Power Sources* **28** 751

Li X F, Xu Y L and Wang C L 2009 *J. Alloys Compd.* **479** 310

Martin C A, Sandler J K W, Shaffer M S P, Schwarz M K, Bauhofer W, Schulte K and Windle A H 2004 *Compos. Sci. Technol.* **64** 2309

Park S C, Kim Y M, Kang Y M, Kim K T, Lee P S and Lee J Y 2001 *J. Power Sources* **103** 86

Pasquier A D, Orsini F, Gozdz A S and Tarascon J M 1999 *J. Power Sources* **81–82** 607

Sakunthala A, Reddy M V, Selvasekarapandian S, Chowdari B V R and Selvin P C 2010 *Electrochim. Acta* **55** 4441

Son J T, Park K S, Kim H G and Chung H T 2004 *J. Power Sources* **126** 182

Thirunakaran R, Kim K T, Kang Y M and Jai Y L 2005 *Mater. Res. Bull.* **40** 177

Tu J, Zhao X B, Cao G S, Tu J P and Zhu T J 2006 *Mater. Lett.* **60** 3251

Xiao L F, Zhao Y Q, Yang Y Y, Cao Y L, Ai X P and Yang H X 2008 *Electrochim. Acta* **54** 545

Yue H J, Huang X K, Lv D P and Yang Y 2009 *Electrochim. Acta* **54** 5363

Zhou W J, Bao S J, He B L, Liang Y Y and Li H L 2006 *Electrochim. Acta* **51** 4701

Zhou W J, He B L and Li H L 2008 *Mater. Res. Bull.* **43** 2285